JOURNAL OF GEOPHYSICAL RESEARCH, VOL. 94, NO. A6, PAGES 6986–6994, JUNE 1, 1989

Lightning as an Embryonic Source of VLF Hiss

VIKAS S. SONWALKAR AND UMRAN S. INAN

STAR Laboratory, Stanford University, Stanford, California

Data from the DE 1 satellite show that lightning-generated whistlers often trigger hiss emissions that endure for up to 10- to 20-s periods. The data consist of the measured electric and magnetic fields in the frequency range of 1.5 kHz to 6.0 kHz, during 22 DE 1 passes during the period December 28, 1986 to January 18, 1987. The 22 passes were nearly identical in terms of their projections on a magnetic meridional plane, and they covered L shells of 3.4 to 5.1 and geomagnetic latitude of 20°N to 40°S in the afternoon (~1400–1500 MLT) sector. The geographic longitudes of the 22 passes were within ±50° of 80°W, and the geomagnetic activity during the period covered was relatively quiet ($\Sigma Kp < 20$ for most of the days). The whistler-triggered hiss emissions were observed on 16 of the passes, and they generally exhibited the following characteristics: (1) emission spectra were wide band (1–2 kHz) and rather structureless, (2) well-defined and sustained fading patterns were observed at twice the spin frequency over 10- to 20-s periods, (3) the spin fading characteristics of the triggered hiss bursts were similar to those reported for background plasmaspheric hiss (Sonwalkar and Inan, 1988), indicating a large wave normal angle with respect to the ambient magnetic field. Our results indicate that lightning-generated whistlers may be an important embryonic source for magnetospheric hiss and that whistlers and emissions triggered by them often constitute the dominant wave activity in the ~1.5- to 6-kHz range on L shells of 3.5 to 5 in the afternoon sector during geomagnetically quiet periods. Through cyclotron and Landau resonant scattering, it is likely that these lightning-generated waves play a dominant role in the loss of ~0.5- to 50-keV electrons trapped on these field lines in the afternoon sector. Through anisotropic proton instability, these waves can also interact with ring current protons in the range of several tens of keV leading to a loss mechanism for ring current protons.

1. INTRODUCTION

Whistler mode waves and their interactions with energetic particles have been a subject of interest since the discovery of the radiation belts. These interactions establish the high levels of ELF/VLF noise in the ionosphere and the magnetosphere and play an important role in the acceleration, transport and loss of energetic particles in planetary magnetospheres [*Kennel and Petschek*, 1966; *Schulz and Lanzerotti*, 1974; *Lyons et al.*, 1972; *Dessler*, 1983]. In the Earth's magnetosphere waves known to interact strongly with particles include chorus and hiss emissions, lightning generated emissions, and man-made signals from VLF transmitters. Of particular interest among these are the steady, incoherent hiss emissions that were identified early on as a dominant contributor to the loss of radiation belt particles [*Kennel and Petschek*, 1966; *Lyons et al.*, 1972]. However, as discussed below, the mechanisms for generation and sustenance of hiss are not yet understood, and recent experimental data suggest that other waves, in particular lightning-generated whistlers, may play an important role in determining the loss rate of energetic particles [*Voss et al.*, 1984; *Inan and Carpenter*, 1987; *Inan et al.*, 1988].

The generation mechanisms of whistler mode hiss remain controversial in spite of an extensive amount of experimental and theoretical work [*Barrington et al.*, 1963; *Dunckel and Helliwell*, 1969; *Russell et al.*, 1969; *Thorne et al.*, 1973; *Kennel and Petschek*, 1966; *Lyons et al.*, 1972; *Thorne et al.*, 1979; *Church and Thorne*, 1983; *Huang et al.*, 1983; *Solomon et al.*, 1988]. *Kennel and Petschek* [1966] provided a theory to explain the existence of stable radiation belts in terms of an equilibrium between the trapped energetic particle flux density and the wideband ELF/VLF whistler mode energy present in the magnetosphere. This theory addressed the question of interactions between the trapped particles and the whistler mode waves near the equilibrium state at which an upper limit can be defined for the magnitude of the stably trapped particle flux density and a corresponding wave magnetic field strength. Many observations have been consistent with the predictions of *Kennel and Petschek* [1966], although energetic electron fluxes that exceed the predicted trapping limit are occasionally observed [*Davidson et al.*, 1988]. While the dynamics of equilibrium state were described by *Kennel and Petschek* [1966], the mechanisms of generation of the observed hiss intensity levels following a nonequilibrium state (when no hiss is present [*Smith et al.*, 1974]) are not understood. After consideration of both cyclotron and Landau resonance interactions, it was proposed that an embryonic source feeds initial energy into the whistler mode hiss [*Church and Thorne*, 1983; *Huang et al.*, 1983]. Once hiss is generated, the gain/loss calculations along the propagation trajectory, involving reflections in the magnetosphere, are sufficient to explain the subsequent maintenance of the hiss at the observed level [*Huang et al.*, 1983]. Recently, *Solomon et al.* [1988] have shown experimentally that amplification of background noise to observed hiss intensities is possible. However, their conclusions are based on limited data sets which are not representative of the average magnetospheric conditions considered by other authors [*Church and Thorne*, 1983; *Huang et al.*, 1983].

Paper number 89JA00392.
0148-0227/89/89JA-00392$02.00

The above mentioned theories of hiss generation [*Kennel and Petschek*, 1966; *Huang et al.*, 1983; *Thorne et al.*, 1973, 1979; *Church and Thorne*, 1983] considered wave-particle interactions involving waves propagating parallel to the geomagnetic field. The main reason behind this assumption has been that the quasi-linear theory put forward by *Kennel and Petschek* [1966] predicts high gain for the parallel propagation and damping for propagation with large wave normals. Recent measurements of wave normal direction(s) of hiss by various authors [*Lefeuvre et al.*, 1983; *Hayakawa et al.*, 1986; *Parrot and Lefeuvre*, 1986; *Sonwalkar and Inan*, 1988] indicate that most often hiss propagates at large wave normal angles with respect to geomagnetic field. Similarly, an earlier study indicated that the band-limited hiss data observed on the low-altitude (400 to 900 km) OGO 4 satellite were consistent with an equatorial source at $L \sim 4$ radiating at large wave normal angles [*Muzzio and Angerami*, 1972]. An alternate mechanism proposed by *Parady* [1974] shows that amplification of the wave propagating at large wave normal angles is possible via the anisotropic proton instability. In particular, Parady shows that an anisotropic ring current proton distribution with a peak at 20 keV is unstable to whistler mode waves propagating above f_{LHR} with large wave normal angles. This instability leads to wave growth and scattering of ring current protons in the loss cone. In view of the recent experimental results, it appears that the mechanism suggested by Parady could play an important role in the magnetospheric generation of hiss.

In this paper we provide new evidence that whistler wave energy introduced into the magnetosphere from atmospheric lightning discharges may be an embryonic source for whistler mode hiss within the plasmasphere. In the past a similar suggestion was made by *Dowden* [1971] based on ground observations of highly dispersed echoing whistlers. An inverse process, that is temporary suppression of preexisting hiss by a whistler and subsequent echoes, was reported by *Gail and Carpenter* [1984].

2. INSTRUMENTATION

The data utilized in this paper were acquired in the course of VLF wave injection experiments carried out during 1986–1987 austral summer using the Stanford University VLF transmitter at Siple Station, Antarctica [*Helliwell and Katsufrakis*, 1974], and the linear wave receiver (LWR) on the Dynamics Explorer (DE 1) satellite. The LWR receiver is integrated into the plasma wave instrument (PWI) on the DE 1 satellite [*Shawhan et al.*, 1981] and measures wave amplitude in three frequency bands: 1.5–3 kHz, 3.0–6 kHz and 10.0–16.0 kHz. The gain of the amplifier can be set at 10-dB steps over a 70-dB range and can be varied automatically or can be commanded to remain fixed at any level. In the automatic mode the gain is reset every 8 s. The response is linear over a 30-dB range in any gain position, thus facilitating accurate measurement of signal intensity and temporal growth rate. The LWR can be commanded to cycle between a 200-m-long electric dipole ($L_{eff} \sim 200$ m) or a 0.8-m by 1.25-m single-turn loop magnetic antenna (threshold sensitivity $6 \times 10^{-10}\ \gamma/(\text{Hz})^{1/2}$ at 6 kHz). The input impedance of the LWR preamplifier is $\geq 10^9\ \Omega$. The LWR allows for detailed quantitative study of phenomena within the passband, providing for measurement of signal growth characteristics as well as spin fading [*Rastani et al.*, 1985; *Sonwalkar and Inan*, 1986]. The antennas on DE 1 satellite can also be connected to a wideband receiver (WBR) with an automatic gain control (AGC) amplifier. WBR has a dynamic range of 100 dB and covers a wide frequency range. However, because of its rapid AGC it is difficult to monitor important features of certain signals which are relatively weak. Another consequence of AGC is to suppress the spin fading effect, which plays a crucial role in our characterization of hiss signals [*Sonwalkar and Inan*, 1988]. The results presented here are based mostly on the data received by LWR. However, during the course of our experiments, the electric field antenna was occasionally switched to WBR in the 0.65- to 10-kHz mode to sample the wideband data. We make use of the data from WBR to qualitatively extend our results below the lower cutoffs (1.5 or 3.0 kHz) of the LWR.

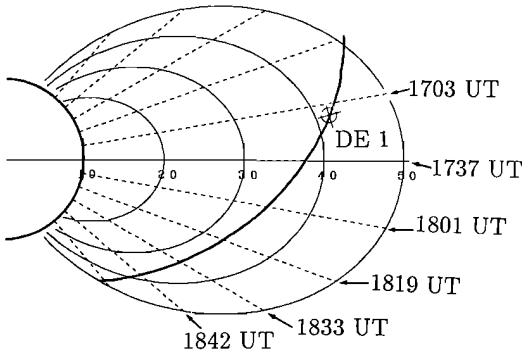

Fig. 1a. Projection of the DE 1 satellite trajectory onto the magnetic meridional plane for January 10, 1987. This trajectory is typical for the period December 28, 1986 to January 18, 1987, during ~1400–1500 MLT when the observations were made.

3. OBSERVATIONS

The observations of broadband hiss emissions triggered by whistlers are based on the measurements of electric and magnetic fields in the frequency range of 1.5 kHz to 6.0 kHz, during 22 DE 1 passes during the period December 28, 1986 to January 18, 1987. Figure 1*a* shows a typical orbit. The 22 passes were nearly identical in terms of their projections on a magnetic meridional plane, and they covered L shells of 3.4 to 5.1 and geomagnetic latitudes of 20°N to 40°S in the afternoon (~1400–1500 MLT) sector. The geographic longitudes of the 22 passes were all within ±50° of 80°W, and the geomagnetic activity during the period covered was relatively quiet ($\Sigma Kp < 10 - 20$ for most of the days, where ΣKp is the daily sum of Kp; see Figure 3). During the 22 passes of interest, the wave data downlinked from the satellite were mostly the 1.5- to 3.0-kHz or 3.0- to 6.0-kHz output from the LWR, and occasionally the 0.65- to 10.0-kHz output from the WBR. DE 1 orbital segments of interest were, for the most part, inside the plasmasphere, as evident from the relatively quiet geomagnetic conditions throughout this period (bottom panel, Figure 3), during which time the plasmapause boundary generally extends beyond L=4–5 [*Carpenter and Park*, 1973].

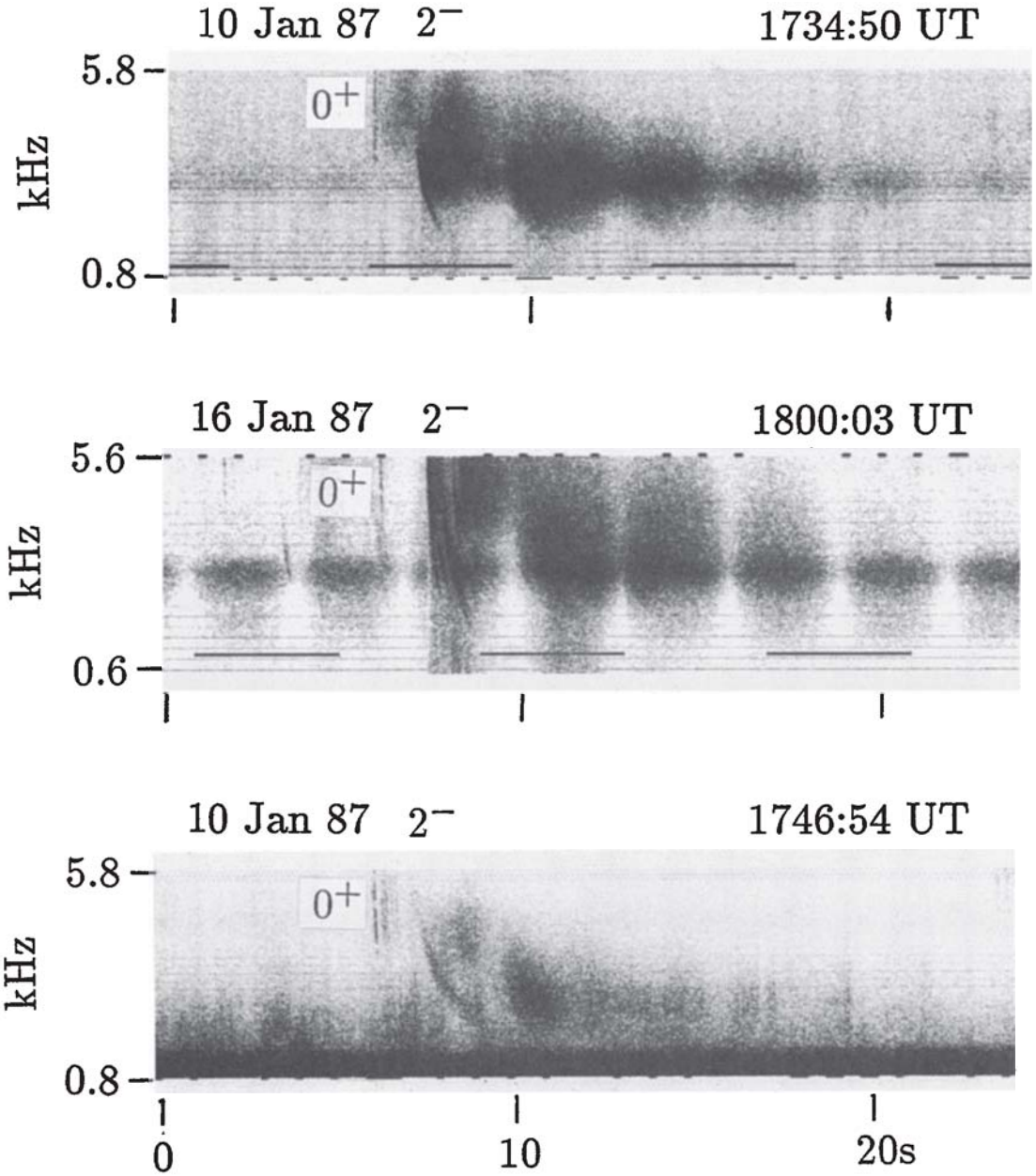

Fig. 1b. Typical signatures of whistler-triggered hiss emissions as received on the LWR (top and the second panel) and WBR (bottom panel).

Examples of Whistler-Triggered Hiss Emissions

Figure 1b shows typical examples of whistler-triggered hiss as received on LWR and WBR. During these times the LWR was in the 3.0- to 6.0-kHz mode, while WBR was in the 0.65- to 10.0-kHz mode. The top panel and the second panel show whistler-triggered hiss as seen by LWR on January 10, 1987, and January 16, 1987, respectively. Based on their dispersion characteristics, the whistler components can be identified as 0^+, 1^-, 1^+, 2^-, etc. [*Smith and Angerami*, 1968]. The components 0^+, 1^- are waves reaching the satellite directly, whereas the components such as 1^+, 2^- are waves reaching the satellite after magnetospheric reflection. We note that (1) the emission endures for ~15–20 s, (2) the spectrum shows the well-defined spin fading characteristic of hiss signals [*Sonwalkar and Inan*, 1988], and (3) hiss is triggered by the second whistler component labeled 2^- and not by 0^+. On January 16, 1987, a weak background hiss band was present throughout. As seen in the middle panel, the phase of spin fading on triggered hiss emissions is the same as that of the background hiss. The third panel shows whistler-triggered hiss emissions observed on the same day (January 10, 1987) and at a similar location as in the top panel, but received on WBR. The difference in the apparent signatures of a similar event (whistler-triggered hiss) by LWR and WBR is evident and is a result of different

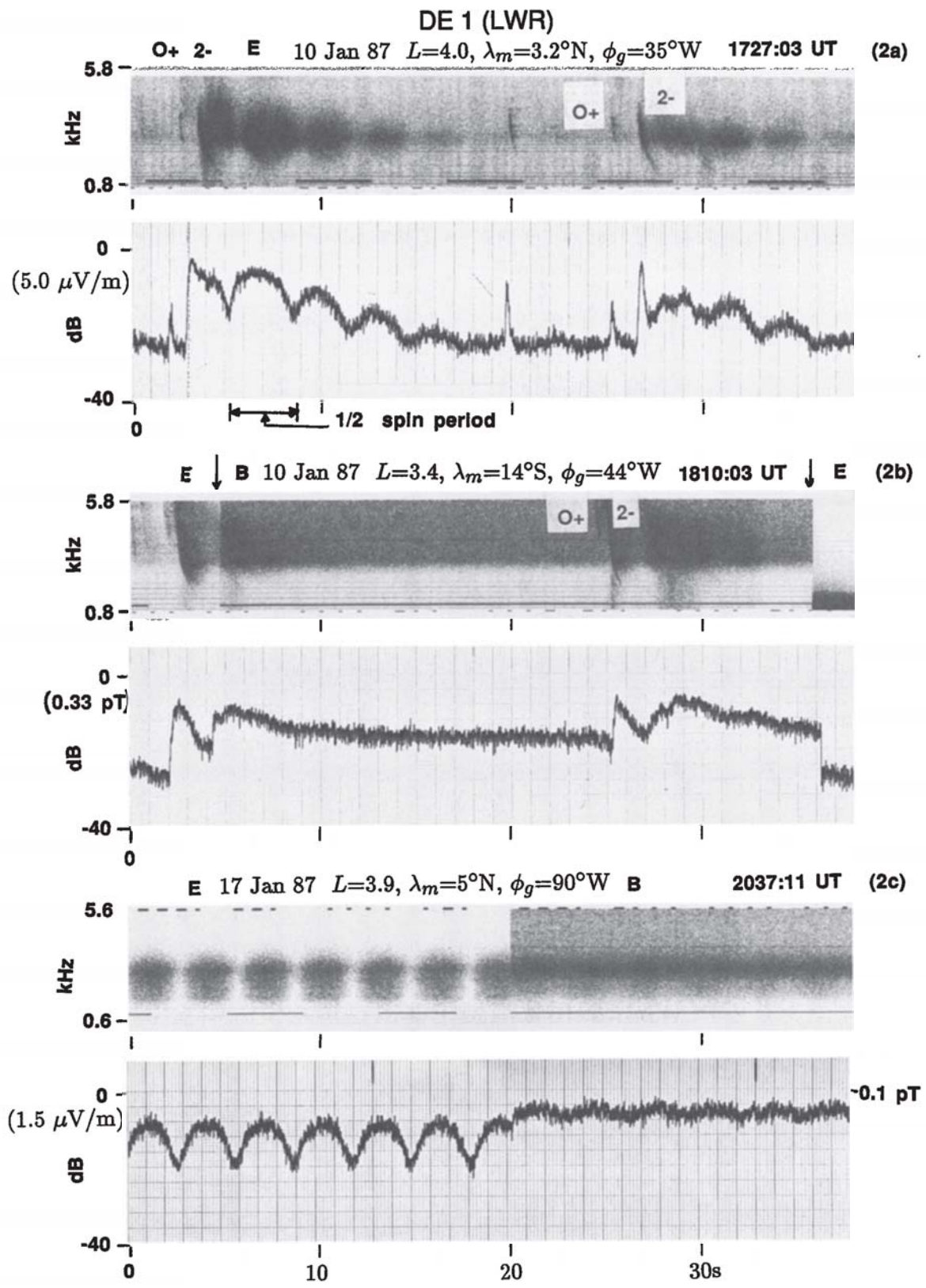

Fig. 2. Examples of observations. (*a*) The spectrogram (upper panel) and the wideband (1 kHz) intensity (lower panel) of the electric field of a whistler-triggered hiss; 0 dB corresponds to 5 μV/m. (it b) The same as Figure 2*a* for the electric (E) and magnetic (B) fields of the whistler-triggered hiss; 0 dB corresponds to 0.33 pT. (*c*) Typical spectrum (upper panel) and the wideband intensity (1 kHz) of the electric and magnetic field of the whistler mode hiss received on the DE 1 satellite on January 17, 1987; 0 dB corresponds to 1.5 μV/m (for electric field) or 0.1 pT (for magnetic field).

characteristics of the receiver as mentioned in the previous section. The signal received by WBR shows emission components below 2.0 kHz and a steady hiss band below 1.0 kHz. On January 10, 1987, we also found that variable frequency signals transmitted from Siple Station, Antarctica, also triggered hiss emissions. While it is interesting to note that the Siple transmitter signals can at times trigger hiss in much the same way as whistlers, in this paper we confine our attention to whistler-triggered hiss. One might ask, why was this phenomenon not noticed on earlier satellites? There are several possible reasons. In the past most satellite VLF receivers were wide band with AGC, similar to WBR on DE 1. These receivers generally track low frequency (<1 kHz) hiss which is much stronger than signals at higher frequency. The condition of suitable satellite orbits over extended values of latitude while keeping in the same L shell ($L \sim 3$–4) and for many days in succession is not easily met in many of the previous missions. Finally the characterization of hiss signals observed by a LWR on a spin-stabilized satellite has only recently been done [*Sonwalkar and Inan*, 1988]; this result is crucial in noticing the similarities between the whistler-triggered hiss and sustained VLF hiss. However, we mention here that emissions similar to the ones reported here were seen by the LWR on ISEE 1 satellite (J. Yarborough, private communication, 1989).

The top panel of Figure 2*a* shows the electric field spectrum of the emission triggered by a whistler, and the lower panel shows the intensity in a 1-kHz-wide band centered at 3250 Hz. (The actual intensity will be somewhat higher due to a ~5-dB/100-Hz filter roll-off for frequencies below 3 kHz, the lower cutoff. This underestimation of the intensity will affect the intensity values quoted in Figures 2*b* and 2*c* in a similar manner.) The figure shows the first whistler component (labeled 0^+) and the magnetospherically reflected component (labeled 2^-) and the subsequent broadband hiss emission enduring for ~10 to 15 s. The apparent lower-frequency cutoff in this figure was set by the LWR receiver, which was operating in the 3.0- to 6.0-kHz band. As shown in Figure 1*b*, the WBR measurement indicates that the emission frequency extended down to ~1 kHz and perhaps even lower. The spectrum of the hiss burst is rather structureless, and the intensity shows the typical well-defined spin fading. Figure 2*b* shows the magnetic field (and electric field in the beginning and end parts) spectrum and the intensity in a 1-kHz-wide band centered at 3250 Hz for a similar event. Note again that the first whistler component does not trigger, while the magnetospherically reflected component does. (The first whistler component is not seen on the intensity chart since it contains frequencies that lie outside the band selected.) The spin fading on the magnetic antenna is much less pronounced than that on the electric field antenna. Figure 2*c* shows an example of hiss observed on January 17, 1987. The orbit on this day was similar to that on the January 10, 1987, and similar geomagnetic conditions existed. While no pronounced whistler activity is evident, a structureless hiss band was observed throughout this pass as seen in Figure 2*c*. The similarity in the electric and magnetic field fading patterns of this hiss and those of whistler-triggered hiss emissions shown in Figures 2*a* and 2*b* is evident. The electric and magnetic field amplitudes of the triggered hiss emissions of Figures 2*a* and 2*b* and those of background hiss of Figure 2*c* are comparable (~1 μV/m and ~0.1 pT, respectively).

General Features

Based on more than 1500 events (whistler triggering of hiss) observed over 16 of the 22 passes, the general features of the phenomenon are noted as follows.

1. The triggered hiss is observed between ~1.5 and 4.0 kHz and appears to have a bandwidth of ~1 to 2 kHz. The center frequency and the bandwidth of the hiss emission remain the same over an entire pass, with the spectrum being rather structureless. The lower frequency limit of 1.5 kHz is set by the LWR lower cutoff, and thus it is likely that the triggered hiss bands extended below 1.5 kHz, and that the bandwidth of the emissions was larger than 2.0 kHz.
2. The individual whistler-triggered hiss emissions generally endured for 10 to 20 s.
3. The hiss emissions were most often triggered by a 1^+ or 2^- whistler (magnetospherically reflected (MR) component) and rarely by a 0^+ or 1^- whistler (the first component of the whistler that arrives at the satellite before going through a magnetospheric reflection). The dispersions of the magnetospherically reflected whistler and the hiss emission are identical, i.e., the arrival times of any particular frequency components of the MR whistler and the triggered hiss are identical (see Figure 1). At times a relatively weaker emission was observed on the first component at frequencies $\geq$4 kHz.
4. The triggered hiss bands exhibited well-defined spin fading patterns. Generally the electric field antenna shows deep fading, whereas the magnetic field antenna shows little or no fading. These fading patterns are similar to those reported for whistler mode hiss observed on the DE 1 satellite [*Sonwalkar and Inan*, 1988] and are indicative of large wave normal angle with respect to the geomagnetic field. On days when there was a weak background hiss band observable (such as shown in the middle panel of Figure 1*b*), the spin fading on whistler-triggered hiss was always in phase with the spin fading on the weak background hiss band. (It may be noted here that spin fading effects are generally separable from dispersion effects because the former have an exact periodicity at twice the spin period.)
5. The electric and magnetic field amplitudes of these emissions and that of background hiss observed on other days along similar trajectories (but in the absence of whistlers) were of the same order of magnitude (within 20 dB).

Occurrence Rates

The top panel of Figure 3 shows the occurrence rate of the triggered hiss bursts and whistlers observed between the geomagnetic equator and 10°S geomagnetic latitude on the different satellite passes. The L values on this part of the orbit ranged between 3.5 and 3.8. For the first 12 passes, from December 27, 1986, to January 8, 1987, the LWR was in the 1.5- to 3.0-kHz mode. For the last 10 passes, from January 9, 1987, to January 18, 1987, the LWR was in the 3.0- to 6.0-kHz mode. In establishing the whistler rate the 0^+ and the subsequent components were treated as one whistler event, since they are interpreted to originate from the same lightning source. The figure also shows the days when almost no whistlers or whistler-triggered hiss emissions were seen. Figure 3 shows that the emissions reported here were found on 16 of the 22 passes. In the 1.5- to 3.0-kHz band it was observed on 7 out of 12 passes, and in the 3.0- to

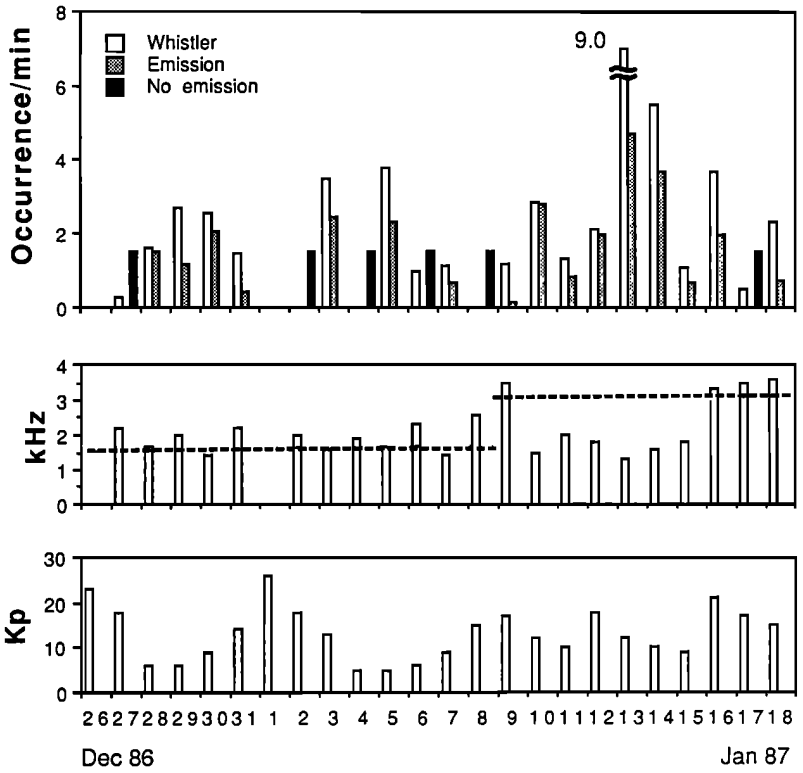

Fig. 3. (Top) Occurrence per minute of whistlers and whistler-triggered hiss between the geomagnetic equator and 10°S latitude for the period December 28, 1986 to January 18, 1987. The solid bar indicates the days when very little or no whistler and emission activity was observed. (Middle) The upper cutoff of hiss signal observed on the same days. The lower cutoff extends below 600 Hz. (Bottom) The geomagnetic activity as given by daily sum ΣKp for the same period.

6.0-kHz band it was observed 9 out of 10 passes. On each of these passes, the WBR output was occasionally downlinked for a few minutes, giving a survey of wideband (0.65 to 10.0 kHz) wave activity. It was observed that a detectable hiss band, generally below 1.5 kHz, was present on the WBR output for each of the passes. The second panel of Figure 3 shows the upper cutoff of the hiss signals. These signals were also observed by LWR, whenever the upper cutoff of the hiss band exceeded the lower cutoff of LWR. On all those days when both background plasmaspheric hiss and whistler-triggered hiss emission were observable on LWR, the hiss was amplified and the phase of spin fading was similar to that for the case shown in the middle panel of Figure 1*b*. The low-frequency (<1.5 kHz) hiss was present even on those days when there were no whistlers and triggered emissions. In general, hiss was found to be the strongest signal below ~1.5 kHz, and the whistlers and the triggered hiss were strongest between 1.5 and 4.0 kHz. The bottom panel shows the ΣKp indicating that the geomagnetic conditions generally remained quiet during this entire period.

Figure 4 presents the average over 22 passes of the rate of occurrence of the triggered hiss events and whistlers as a function of the geomagnetic latitude and the corresponding L shell. Table 1 gives the numerical data corresponding to Figure 4. The average rate of whistlers, the triggered emissions and the ratio of triggered hiss emissions to whistlers are lower for the latitude ranges between 20°N and the geomagnetic equator. For the DE 1 orbital segments studied, latitude > 5°N corresponds to $L > 4$. Occurrence rates are higher for southern latitudes between the geomagnetic equator and 40°S, where the corresponding L shell range was 3.3–4.0. The relative rate of occurrence for the triggered emissions observed south of the geomagnetic equator was nearly constant (~ 0.65). The bottom line of the abscissa

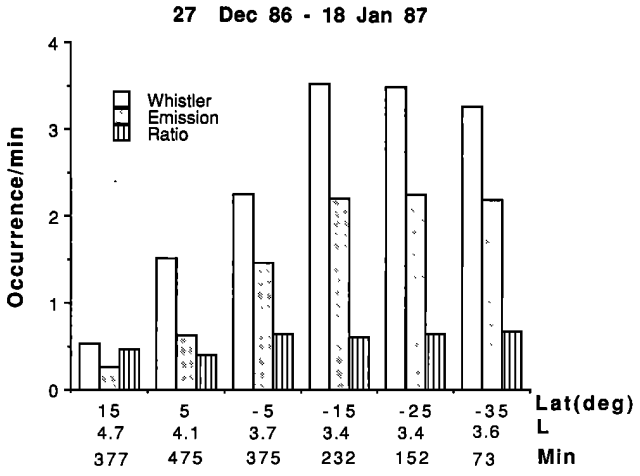

Fig. 4. The average occurrence/min of whistlers and the triggered hiss emissions as a function of the geomagnetic latitude. The figure also gives the ratio of the occurrences of the hiss emissions and whistlers. The lowest panel of the x axis gives the net time in minutes the data were collected in each latitude segment.

TABLE 1. Occurrence Rate per Minute as a Function of Geomagnetic Latitude and L Shells

	20°N–10°N $L = 4.7$	10°N–0° $L = 4.1$	0°–10°S $L = 3.7$	10°S–20°S $L = 3.4$	20°S–30°S $L = 3.4$	30°S–40°S $L = 3.6$
Whistler	0.54	1.52	2.26	3.54	3.50	3.28
Emission	0.25	0.63	1.47	2.21	2.26	2.20
Ratio	0.46	0.41	0.65	0.62	0.65	0.67

in Figure 4 shows the total time over which the data were averaged for each latitude segment. The net time in minutes that data were collected in different latitude segments varied as a result of the elliptical orbit of the satellite.

4. Discussion

We now discuss the implications of our observations from several different perspectives. Firstly, our data suggest that in the frequency range 1.5 to 6.0 kHz, in the afternoon section, during relatively quiet conditions, whistlers and triggered broadband hiss are the dominant wave activity inside the plasmasphere between $L = 3.3$–4.0. This result was found to be the case for 16 of the 22 passes analyzed. From Figure 4 we see that inside the plasmasphere ($L \leq 4$), we observe ~3 whistlers and ~2 emissions per minute. Taking 10 to 15 s as the average length of the emission, we see that the duty cycle is about 30–50%. Below ~1.5 kHz, plasmaspheric hiss was observed to be present on all of the 22 passes. This steady background hiss was generally confined to frequencies < 2 kHz, but the upper cutoff exceeded 3 kHz or more on a few occasions. Assuming that waves are propagating at the Gendrin angle [*Gendrin*, 1961], electron density 500 el/cm^3 and L=4, the cyclotron resonant energy is inversely proportional to the square of the frequency and is 45 keV at f =1.5 kHz. The corresponding electron energies for Landau resonance interactions would be nearly independent of wave frequency and are about ~0.6 keV. In view of this, we can expect that in the L shell range of 3.3–4, whistlers and whistler-triggered hiss emissions may play an important role in the loss of radiation belt particles with energies $\leq$ 45 keV. As mentioned in the introduction these waves can also interact with ring current protons of several tens of keV via anisotropic proton instability [*Parady*, 1974].

A second issue we wish to consider is the role lightning plays in the generation and/or amplification of hiss. At the outset, we note a few points of general relevance.

1. VLF hiss and whistlers are both common phenomena and are limited predominantly to the inner magnetosphere (plasmasphere) [*Thorne et al.*, 1973; *Edgar*, 1972].

2. Typically the frequency band of whistlers ranges from a few hundred hertz to 10 kHz, and that of hiss ranges from a few hundred hertz to 3–4 kHz.

3. Whistlers are known to interact with the radiation belt particles [*Voss et al.*, 1984]. Theoretical calculations in the past have suggested that hiss may be playing a dominant role in the precipitation of energetic particles [*Lyons et al.*, 1972].

4. Most of the whistler energy injected from the ground due to lightning remains trapped in the magnetosphere due to magnetospheric reflections. These trapped waves generally make large wave normal angles with respect to the geomagnetic field [*Smith and Angerami*, 1968; *Edgar*, 1972]. Since collisions are negligible, these waves in the long run can only be damped or amplified as a result of wave-particle interactions.

5. Based on the amplification (cyclotron) and damping (Landau) calculations along the ray paths for magnetospheric hiss, *Huang et al.* [1983] and *Church and Thorne* [1983] have concluded that these mechanisms cannot explain generation of hiss from the background thermal radiation.

To this general picture we add our observations from the DE 1 data:

1. Whistlers trigger emissions inside the plasmasphere at a fairly high rate.

2. The emissions are broadband, below ~4 kHz, and their spectrum is rather structureless.

3. The triggered hiss emissions show spin fading similar to that reported earlier for hiss [*Sonwalkar and Inan*, 1988]. The spin fading patterns provide data on wave normal directions. In this case they indicate large wave normal angles. On those days when the triggered emissions and hiss were observed simultaneously, the phase of the fading is identical for whistler-triggered hiss and background hiss.

4. The intensity of triggered hiss is comparable to that of background VLF hiss observed in the same frequency band during similar periods.

By combining these factors we arrive at a strong possibility that lightning energy introduced in the magnetosphere may be an embryonic source of plasmaspheric hiss. There are two possible ways by which the final production of continuous hiss might take place. In the first, whistler-triggered emissions along with the first MR component of the whistler undergo multiple magnetospheric reflection and fill up the plasmasphere with radiation that has the appearance of hiss. (It is possible that additional emissions are generated during each trip across the equator.) Alternatively, the whistler-triggered emissions lead only to an initial weak hiss, which undergoes further amplification so as to reach the observed hiss intensity. We note the fact that on 6 days when there were no whistlers and no triggered emissions, a hiss band was still present. This observation implies that the hiss can sustain itself in the absence of whistlers and is consistent with the view that whistlers initially feed energy into the magnetosphere in the form of whistler triggered hiss which is further amplified enough to reach the observed levels. We now turn to the question of why hiss is generally observed below 1.5 kHz, while the-triggered hiss emissions go up to 4.0 kHz. The answer comes from ray tracing studies. After tracing rays injected at ionospheric heights at various latitudes between 20° and 60° and wave frequencies between 0.5 kHz and 4 kHz (for 30 s of group delay), we found that in general, rays of frequencies below 1.5 kHz eventually (af-

ter 3–4 reflections) reach an L shell of 3 to 4 and remain trapped there due to magnetospheric reflections. The rays with higher frequencies generally settle down at L shells of 3.0, and lower. *Lyons and Williams* [1984] pointed out that, irrespective of the details of energetic particle distribution, the favored interaction region is at higher L shells ($L \sim 4$) that lie just within the plasmasphere. The foregoing conclusion is based on the facts that (1) due to the lowest magnetic energy per particle ($B^2/8\pi N$) in this region, lower-energy particles interact with the waves and that (2) the particle flux typically increases with decreasing energy. Thus, the lower-frequency waves that reach higher L shells and spend more time in the favorable interaction region lead to the generation of sustained hiss. This qualitatively explains why sustained hiss is observed more often at frequencies below ~1.5 kHz. At this point we note that the sustained hiss below ~1.5 kHz is generally an order of magnitude more intense than triggered hiss emissions or sustained hiss observed at frequencies above ~1.5 kHz. This is indicated by the WBR spectrogram in the bottom panel of Figure 1*b* and also by typical hiss spectra such as those shown in *Huang et al.*, [1983].

The next question we discuss is the location and nature of the wave-particle interactions. Our observations suggest that the source is localized near $L \sim 4$ in the equatorial plane. This conclusion is based on (1) the fact that the emission spectrum (center frequency and bandwidth) is independent of latitude and (2) the fact that the ratio of the rate of triggered hiss emissions to that of whistlers is independent of latitude and drops for $L > 4$ (Figure 4). Our analysis also suggests that wave-particle interactions involve waves propagating with large wave normal angle with respect to the geomagnetic field. This result is based on (1) large wave normal angles indicated by the spin fading pattern, (2) the fact that the emission is triggered by the magnetospherically reflected component, and (3) the fact that the dispersion seen on the magnetospherically reflected whistlers and the generated emissions is identical, implying that both the whistler and the noise burst have propagated with similar (and large) wave normal angles. These two results, namely, interaction region and large wave normal angles, are also consistent with the hiss source described in a previous paper [*Sonwalkar and Inan*, 1988]. An interesting point to note is that when the waves propagate at high wave normal angles close to the Gendrin angle, the group ray direction is parallel to the geomagnetic field and the ray remains confined to the same L shell over a relatively large range in latitude. As a result, the duration of the resonant interaction with particles of the same energy range is enhanced. Finally we note that since the lightning-generated whistlers have to propagate through the ionosphere before reaching magnetospheric altitudes, direct multiple path propagation may play a significant role in determining the actual wave structure that interacts with the particles. Consequences of multiple path propagation for wave-particle interactions are (1) that a cyclotron (or Landau) resonant electron will experience a wave Doppler broadening of a few tens of hertz to a few hundreds of hertz, leading to a larger number of particles interacting with the wave, and (2) reduced coherence length leading to generation of broadband noises [*Sonwalkar et al.*, 1984].

In conclusion we note the role of lightning in the magnetospheric wave-particle interactions and radiation belt dynamics. The data shown in this paper indicate that there is a strong possibility that lightning is an important source of hiss, at least in the embryonic sense. Other experimental evidence has been interpreted to suggest that whistler mode hiss could be a cause of VLF chorus [*Koons*, 1981; *Helliwell et al.*, 1986]. Therefore it appears that the wave energy introduced in the magnetosphere by atmospheric lightning discharges may play an important role not only in the loss of particles through wave-induced precipitation, but also in embryonic generation of hiss.

Acknowledgments. We thank our colleagues in the STAR Laboratory, in particular, R. A. Helliwell, D. L. Carpenter, L. R. O. Storey, T. F. Bell, and J. Yarbrough for many useful comments and discussions. The spectrograms and amplitude charts were produced by J. Yarbrough. We thank R. A. Hoffman for his support of the Stanford University DE 1 program. This research was supported by NASA under grant NAG5-476 at Stanford University.

The editor thanks R. R. Anderson and M. Parrot for their assistance in evaluating this paper.

REFERENCES

Barrington, R. E., J. S. Belrose, and D. A. Keeley, Very low frequency noise bands observed by the Alouette 1 satellite, *J. Geophys. Res., 68*, 6539, 1963.

Carpenter, D. L., and C. G. Park, On what ionospheric workers should know about the plasmapause-plasmasphere, *Rev. Geophys., 11*, 133, 1973.

Church, S. R., and R. M. Thorne, On the origin of plasmaspheric hiss: Ray path integrated amplification, *J. Geophys. Res., 88*, 7941, 1983.

Davidson, G. T., P. C. Filbert, R. W. Nightingale, W. L. Imhof, J. B. Reagan, and E. C. Whipple, Observation of intense trapped electron fluxes at synchronous altitudes, *J. Geophys. Res., 93*, 77, 1988.

Dessler, A. J., *Physics of the Jovian Magnetosphere*, Cambridge University Press, New York, 1983.

Dowden, R. L., Distinction between mid latitude VLF hiss and discrete emissions, *Planet. Space Sci., 19*, 374, 1971.

Dunckel, N., and R. A. Helliwell, Whistler mode emissions on the OGO 1 satellite, *J. Geophys. Res., 74*, 6731, 1969.

Edgar, B. C., The structure of the magnetosphere as deduced from magnetospherically reflected whistlers, Ph.D. dissertation, Stanford University, Stanford, Calif., April 1972.

Gail, W. B., and D. L. Carpenter, Whistler induced suppression of VLF noise, *J. Geophys. Res., 89*, 1015, 1984.

Gendrin, R., Le guidage des whistlers par le champ magnetique, *Planet. Space Sci., 5*, 274, 1961.

Hayakawa, M., M. Parrot, and F. Lefeuvre, The wave normals of ELF hiss emissions observed on board GEOS 1 at the equatorial and off-equatorial regions of the plasmasphere, *J. Geophys. Res., 91*, 7989, 1986.

Helliwell, R. A., and J. P. Katsufrakis, VLF wave injection experiment into the magnetosphere from Siple station, Antarctica, *J. Geophys. Res., 79*, 2511, 1974.

Helliwell, R. A., D. L. Carpenter, U. S. Inan, and J. P. Katsufrakis, Generation of band-limited noise using the Siple Transmitter: A model for magnetospheric hiss, *J. Geophys. Res., 91*, 4381, 1986.

Huang, C. Y., C. K. Goertz, and R. R. Anderson, A theoretical study of plasmaspheric hiss generation, *J. Geophys. Res., 88*, 7927, 1983.

Inan, U. S., and D. L. Carpenter, Lightning induced electron precipitation events observed at L=2.4 as phase and amplitude perturbations on subionospheric VLF signals, *J. Geophys. Res., 92*, 3293, 1987.

Inan, U. S., W. C. Burgess, T. G. Wolf, D. C. Shafer, and R. E. Orville, Lightning-associated precipitation of MeV electrons from the inner radiation belt, *Geophys. Res. Lett., 15*, 172, 1988.

Kennel, C. F., and H. E. Petschek, Limit on stably trapped particle fluxes, *J. Geophys. Res.*, *71*, 1, 1966.

Koons, H. C., The role of hiss in the magnetospheric chorus emissions, *J. Geophys. Res.*, *86*, 6745, 1981.

Lefeuvre, F., M. Parrot, L. R. O. Storey, and R. R. Anderson, Wave distribution functions for plasmaspheric hiss observed on board ISEE 1, *Tech. Note LPCE/6*, Lab. de Phys. et Chim. de l'Environ., Orleans, France, 1983.

Lyons, L. R., and D. J. Williams, *Quantitative Aspects of Magnetospheric Physics*, p. 231, D. Reidel, Boston, 1984.

Lyons, L. R., R. M. Thorne, and C. F. Kennel, Pitch angle diffusion of radiation belt electrons within the plasmasphere, *J. Geophys. Res.*, *77*, 3455, 1972.

Muzzio, J. L. R., and J. J. Angerami, OGO 4 observations of extremely low frequency hiss, *J. Geophys. Res.*, *77*, 1157, 1972.

Parady, B. K., Anisotropic proton instability magnetospheric (APIM) hiss: An introduction, *Geophys. Res. Lett.*, *1*, 235, 1974.

Parrot, M., and F. Lefeuvre, Statistical study of the propagation characteristics of ELF hiss observed on GEOS-1, inside and outside the plasmasphere, *Ann. Geophys., Gauthier Villars, Ser. A*, *5*, 363, 1986.

Rastani, K., U. S. Inan, and R. A. Helliwell, DE 1 observations of Siple transmitter signals and associated side bands, *J. Geophys. Res.*, *90*, 4128, 1985.

Russell, C. T., R. E. Holzer, and E. J. Smith, OGO 3 observations of ELF noise in the magnetosphere, 1, Spatial extent and frequency of occurrence, *J. Geophys. Res.*, *74*, 755, 1969.

Schulz, M., and L. J. Lanzerotti, Particle diffusion in the radiation belts, in *Physics and Chemistry in Space*, edited by J. G. Roederer, p. 96, Springer-Verlag, New York, 1974.

Shawhan, S. D., D. A. Gurnett, D. L. Odem, R. A. Helliwell, and C. G. Park, The plasma wave and quasi-static electric field instrument (PWI) for Dynamic Explorer–A, *Space Sci. Instrum.*, *5*, 535, 1981.

Smith, E. J., A. M. A. Frandsen, B. T. Tsurutani, R. M. Thorne, and K. W. Chan, Plasmaspheric hiss intensity variation during magnetic storms, *J. Geophys. Res.*, *79*, 2507, 1974.

Smith, R. L., and J. J. Angerami, Magnetospheric properties deduced from OGO 1 observations of ducted and nonducted whistlers, *J. Geophys. Res.*, *73*, 1, 1968.

Solomon, J., N. Cornilleau-Wehrlin, A. Korth, and G. Kremser, An experimental study of ELF/VLF hiss generation in the Earth's magnetosphere, *J. Geophys. Res.*, *93*, 1839, 1988.

Sonwalkar, V. S., and U. S. Inan, Measurement of Siple transmitter signals on the DE 1 satellite: Wave normal direction and antenna effective length, *J. Geophys. Res.*, *91*, 154, 1986.

Sonwalkar, V. S., and U. S. Inan, Wave normal direction and spectral properties of whistler mode hiss observed on the DE 1 satellite. *J. Geophys. Res.*, *93*, 7493, 1988.

Sonwalkar, V. S., T. F. Bell, R. A. Helliwell, and U. S. Inan, Direct multiple path magnetospheric propagation: A fundamental property of the VLF nonducted waves, *J. Geophys. Res.*, *89*, 2823, 1984.

Thorne, R. M., E. J. Smith, R. K. Burton, and R. E. Holzer, Plasmaspheric hiss, *J. Geophys. Res.*, *78*, 1581, 1973.

Thorne, R. M., S. R. Church, and D. J. Gorney, On the origin of plasmaspheric hiss: The importance of wave propagation and plasmapause, *J. Geophys. Res.*, *84*, 5241, 1979.

Voss, H. D., W. L. Imhof, M. Walt, J. Mobilia, E. E. Gaines, U. S. Inan, R. A. Helliwell, D. L. Carpenter, J. P. Katsufrakis, and H. C. Chang, Lightning induced electron precipitation, *Nature*, *312*, 740, 1984.

U. S. Inan and V. S. Sonwalkar, Stanford University, STAR Laboratory, Department of Electrical Engineering/SEL, Durand 324, Stanford, CA 94305.

(Received November 21, 1988;
revised February 16, 1989;
accepted February 22, 1989.)